Table of Contents

List of Figures ..... **iv**

List of Tables ..... **iv**

List of Abbreviations ..... **v**

Chapter 1. Introduction **1**

1.1 Objectives of the study *1*

Chapter 2. Literature Review **2**

2.1 Energy efficiency in buildings *2*

2.2 Green energy building technologies *2*

2.2.1 Passive design 2

2.2.1.1 Passive solar heating 2

2.2.1.2 Passive solar cooling 3

2.2.2 Energy-efficient equipment 3

2.2.3 Integrating renewable energy technologies 3

2.3 Quantitative indicators of thermal comfort *3*

2.3.1 Steady-state approach 3

2.3.2 Adaptive comfort approach 4

Chapter 3. Methodology **6**

3.1 Dimensions of the Building *6*

3.2 Collection of Data *7*

3.3 Conduction and convection heat transfer *8*

3.3.1 Calculation of resistance for wall 9

3.4 Ventilation and infiltration heat transfer *9*

3.5 Radiative heat transfer *9*

3.5.1 Opaque surface 9

3.5.2 Glazed surface 9

3.6 Internal heat generation *10*

3.7 Energy balance *10*

3.8 Load Requirements *11*

3.8.1 Control System 11

Chapter 4. Sizing and selection of the energy production plants **13**

4.1 PV panel-based energy production plant (System A) *13*

4.2 Specifications of the components *13*

4.3 Solar collector-based energy production plant (System B) *14*

4.4 Specifications of the components *14*

4.5 Optimization *15*

4.5.1 Optimization algorithm of PV Plant (System A) 15
4.5.2 Optimization algorithm of the solar collector plant (System B) 16
4.6 Optimization Results *18*
Comparison of system A and system B *19*
4.6.1 Levelized energy cost 19
4.6.1.1 Methodology of LCOE, LCOC & LCOH Calculation 19
4.6.1.2 Capacity Utilization Factor 21
4.6.2 Break-even point/payback time 21
4.6.3 Carbon Savings 22
Chapter 5. Conclusion 23
Chapter 6. Bibliography 24
Appendix A 27
Building Drawings, Dimensions, and Material Properties 27

List of Figures

Figure 1 Expected evolution of air conditioning load in future 1
Figure 2 Thermal sensation scale 4
Figure 3 PPD as a function of PMV 4
Figure 4 Dimensions of the building 6
Figure 5 Satellite Image of the Office Building 7
Figure 6 Solar Irradiance for average day of each month of the Selected Location 7
Figure 7 Ambient temperature profile of an average day of each month 8
Figure 8 Resistances of facade wall (L1) 8
Figure 9 Room temperature without HVAC 11
Figure 10 HVAC load Curve 12
Figure 11 Effect of HVAC on the temperature 12
Figure 12 PV panel and heat pump-based energy production plant 13
Figure 13 Solar collector and absorption chiller-based energy production plant 14
Figure 14 Control strategy applied on PV plant 16
Figure 15 Control strategy applied on solar thermal plant 17
Figure 16 Optimization of system A with batteries 18
Figure 17 Optimization of system B with Thermal Storage 19
Figure 18 Share of each factor in System A total cost 20
Figure 19 Share of each factor in System B cost 20
Figure 20 Break-Even analysis of both the plants 22

List of Tables

Table 1 Areas of different Sides 6
Table 2 Heat sources of the building 10
Table 3 Technical comparison for absorption chiller 15
Table 4 Optimization results 18
Table 5 Costs associated with both plants 20
Table 6 CUF of each system 21
Table 7 Carbon footprint of each system ..... Error! Bookmark not defined.

List of Abbreviations

ASHRAE	American Society of Heating, Refrigerating and Air-Conditioning Engineers
ATAHP	Air to Air Heat Pump
BEP	Break-Even Point
COP	Coefficient of Performance
CUF	Capacity Utilization Factor
EER	Energy Efficiency Ratio
HVAC	Heating, Ventilation, and Air Conditioning
IEA	International Energy Agency
LCOC	Levelized Cost of Cooling
LCOE	Levelized Cost of Energy
LCOH	Levelized Cost of Heating
PV	Photovoltaic
PVGIS	Photovoltaic Geographical Information System
SOC	State of Charge
STC	Standard Temperature Conditions

Executive Summary

The project was intended to design a sustainable and efficient green heating/cooling system for a building in Terrassa, Barcelona. The design was aimed at reducing the overall energy consumption of the HVAC system while also ensuring the required comfort conditions of the room. To achieve this, two different systems were designed and analyzed. The first system (System A) utilized PV panels to generate electrical energy that was used to power a heat pump to produce the heating or cooling demand for the building as required. In addition, the system incorporated batteries for storing energy. On the other hand, the second system (System B) was composed of solar thermal collectors for thermal energy generation, a thermal storage tank for energy storage, and an absorption chiller for cooling and heating directly from the thermal tank. A genetic algorithm was implemented in MATLAB to optimize the required quantities of each of the plant components. The comparison was studied based on the levelized energy cost, breakeven point, utilization factor, and carbon savings with an assumption that the lifespan of both plants were 25 years.

The comparison showed that the characteristics of System A over its lifespan were preferable economically and had a bit shorter break-even period of 16 years compared to that of system B which was 17 years. The results showed that the investment costs between the two systems were also significantly different, which was about 25 percent less for System A, compared to system B.

Chapter 1. Introduction

Throughout the last decade, global efforts have been made to reduce the very dependence on fossil fuels by devising and maturing green energy technologies, thus reducing the global carbon emissions and preserving the fossil fuels. In light of the present hour, the exacerbating climate conditions and its successive impacts on billions of lives and the course of the global economy, it is high time that the major consumers of energy must be gradually shifted toward green technologies.

Having said that, as per the statistics published by the International Energy Agency (IEA), buildings consume one-third of the global energy produced, and one-tenth of the energy is consumed only by the heating and cooling systems [1]. In another report published by the IEA, out of the total energy-related CO_2 emissions, 28% emissions are from buildings.

But the fact is that most homes in hot and densely populated countries like Pakistan, India, etc have not even installed their first AC. Therefore, the cooling or heating systems are only used in a small number of developed countries. Thus, it is obvious that there is going to be a huge increase in the energy consumption for air conditioning around the world as shown in Figure 1.

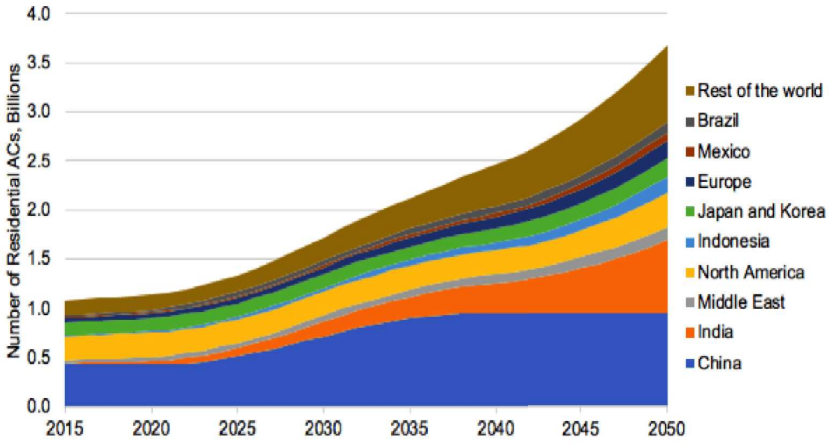

Figure 1 Expected evolution of air conditioning load in future [1]

Therefore, there is a clear and imperative necessity of developing better and more efficient cooling systems. The objective must be to guarantee healthy and adequate environmental conditions for everyone around the world but sustainably without harmful consequences for the environment and world climate.

1.1 Objectives of the study

The objective of this study is to design a green cooling and heating system for a building by analyzing two different solar-based technologies i.e. Solar photovoltaic and Solar thermal system, to make the building's heating and cooling independent of the main grid without compromising the human comfort needs. To conduct this study an office building located in Terrassa, Spain has been chosen.

Chapter 2. Literature Review

To improve the sustainability of buildings and their energy efficiencies, the World Green Building Council noted that research and implementation of alternative ways in which buildings are designed are of great importance, and green buildings are one of such building designs necessary for efficient energy management [2]. Khan et al. concluded that green buildings are a solution to the challenges of global warming as they limit the degradation of natural resources by the efficient use of water and energy to reduce pollution and energy consumption using green energy sources [3].

2.1 Energy efficiency in buildings

Chel and Kaushik reviewed the important contributors to efficient buildings which they summarized as zero energy passive building, low energy building materials, using low energy equipment, and integration of renewable energy technologies [4]. This suggests the importance of energy-efficient equipment and optimizing the renewable energy sources mix. However, achieving energy efficiency in buildings could be challenging as constraints would have to be applied to the building design. Aksamija [5] explored possibilities of improving net-zero energy goals to existent buildings and from energy modeling and simulations concluded that in addition to improving the building's envelop, retrofitting of the HVAC and lighting systems is effective.

2.2 Green energy building technologies

2.2.1 ***Passive design***

This is an important way of improving a building's energy efficiency and this approach can be applied to both existing and new architectures [6]. It requires strategies that would enable high levels of thermal comfort and energy efficiency by use of the local weather which reduces the need for additional heating and cooling. Authors like Borrallo-Jiménez et al. [7] gave criteria that a passive design must meet comprising the space heating demand, primarily renewable energy demand, air tightness, and thermal comfort. Passive designs are usually in form of passive solar heating or passive solar cooling.

2.2.1.1 Passive solar heating

As highlighted by Chel and Kaushik [4], for passive solar buildings, design should involve knowledge of solar irradiation, window technology, and local climate which maximizes the solar illumination obtained during the daytime. This reduces the need for internal illumination. They recommend solar heating which entails the capture of energy from the sun for absorption, storage (in thermal masses), and distribution of its heat. There are three approaches to passive solar heating systems which are direct gain, indirect gain, and isolated gain.

In direct gain, the solar radiation is directly transmitted into the space in the room and the thermal energy is stored in thermal masses which can be used later during the night. As described by the authors [4] for indirect gain, the thermal mass is located between the sun and the room. Using thermal mass, absorbed heat from solar energy is further transferred to the room via conduction and convection. In isolated gain, sunlight is collected in an area that can be separated from the rest of the building. The doors or windows between this living space and the building are opened during the day to circulate collected heat and then closed at night, allowing the temperature to drop. In their review, Chel and Kaushik stated that direct gain utilizes 60 to 75% of solar energy, indirect gain 30 to 35%, and isolated gain 15 to 30% [4].

2.2.1.2 Passive solar cooling

Kamal [8] critically analyzed different passive cooling technologies and established that these techniques can reduce the peak cooling load in buildings, which invariably reduces the size of the air conditioning equipment and the period for which it is generally required. The author further added that reducing the rate of heat gain in the building and encouraging the removal of excess heat from the building would help to maintain a comfortable environment. Two conditions are needed for passive cooling: the availability of a heat sink (this should be lower than the indoor temperature) and the promotion of heat transfer towards the sink [8]. Passive solar cooling can be achieved through solar shading, insulation, radiative and evaporative cooling.

2.2.2 Energy-efficient equipment

Belussi et al. [9] review highlighted the effect of HVAC systems and they account for half of the building's total energy consumption. Thus, they stressed the importance of using innovative materials such as Phase Chase Materials (PCM), thermal energy storage, and recovery of exhaust heat in integrating the performances of systems such as HVAC, domestic hot water, ventilation, radiant floor heating, chilled ceiling, or solar cooling facilities. For energy consumption involving lighting, Cao et. al [6] explained the high contribution of lighting for almost half of the electricity demand of buildings. They further suggested the use of Light Emitting Diodes (LEDs) to this end. However, they noted that 75–85% of the light electric power consumed by LEDs generates convective heat which would require more cooling load. Thus, advanced lighting technologies and daylight harvesting strategies were proposed as additional alternatives. Additionally, Cabeza et al. [10] reviewed and showed the trends of electricity consumed by appliances. They recommended the use of energy-efficient appliances.

2.2.3 Integrating renewable energy technologies

Using renewable energy technologies gives an additional benefit for achieving energy efficiency. Belussi et al. [9] enlisted the exploitation of solar, geothermal, wind, and bioenergy as being fundamental for green energy buildings. Chel and Kaushik [4] explained the systems adopted worldwide to integrate solar energy into buildings. Some of which are solar collectors with absorbers, Fresnel lenses, hybrid photovoltaic/thermal systems, and integration of solar/wind systems. They further elucidated that the integration of solar and wind energy systems is amongst the most interesting renewable energy technologies. Façades and rooftops are suitable for solar systems and small wind turbines can be mounted on rooftops.

2.3 Quantitative indicators of thermal comfort

ASHRAE defined thermal comfort as "the condition of mind that expresses satisfaction with the thermal environment" [11]. As such, thermal comfort varies between persons because of psychological and physiological differences. The primary factors that affect thermal comfort are air temperature, radiant temperatures, relative air velocity, relative humidity, metabolic rate, and thermal resistance of clothing. ASHRAE [12] and Djongyang et al. [13] classified the different approaches to thermal comfort as the steady-state approach and the adaptive comfort approach.

2.3.1 Steady-state approach

The steady-state models are developed to describe human responses to the thermal conditions in situations where the environmental and physiological parameters are quasi-constant in time. Several authors [14], [13]- [15]explain the Fanger heat balance model that is accompanied by

a thermal sensation model based on two indexes, the Predicted Mean Vote (PMV) and the Predicted Percentage of Dissatisfied (PPD).

Orosa [16] described in his review that the PMV model is an evaluation of generic comfort conditions based on the six thermal comfort indicators. It uses a seven-point scale to predict the average value of votes of a group of people which states their thermal sensation. The scale ranges from -3 (too cold) to +3 (too hot) as shown below:

Figure 2 Thermal sensation scale [17]

Enescu [14] described that the PPD model was introduced to predict the number of persons dissatisfied and their level of dissatisfaction based on a certain thermal comfort. Thus, if a particular thermal sensation is chosen, we can verify the number of persons that are dissatisfied with the results.

The relationship between PMV and PPD is given as follows:

$$PPD = 100 - 95e^{[-(0.03353\ PMV^4 + 0.2179\ PMV^4)]} \quad (1)$$

where the dissatisfied persons are persons that do not vote for either +1, 0, or -1 [12].

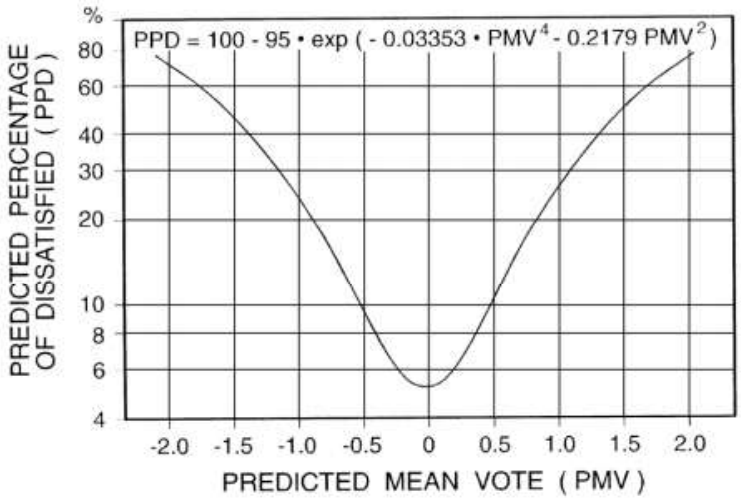

Figure 3 PPD as a function of PMV. [11]

Djongyang et al. illustrated that when PMV = 0, 5% of persons still feel dissatisfied. This is due to variations in how several individuals evaluate their thermal comfort. The recommended acceptable PMV range for thermal comfort from the ASHRAE Standard 55–2010 is −0.5 < PMV < +0.5, corresponding with PPD < 10% for an indoor space [14].

2.3.2 Adaptive comfort approach

In situations where the occupants are under spatially varying thermal conditions such as naturally ventilated buildings, Ma et al [18] described that the PMV index is not recommended because of a large discrepancy between the predicted PMV and the actual thermal sensation

votes. In addition, Orosa [16] noted that a 1.4°C margin of error can be obtained from the PMV model after a neutral temperature has been obtained.

In the review, Djongyang et al. [13] highlighted the adjustments included in the adaptive method. They were summarized in three categories: behavior adaptation, physiological adaptation, and psychological adaptation. One of the adaptive approaches incorporates a mean outdoor effective temperature as an input. In their book [19], Humphrey and Nicol showed that there is a relation between the outdoor monthly mean temperature and the indoor comfort temperature. For a heated or cooled building, the authors developed a model that could predict the likely comfort temperature when the outdoor temperature is known. This can be expressed by:

$$t_c = 23.9 + 0.295(t_{out} - 22)\exp\left[-\left(\frac{t_{out}-22}{20\sqrt{2}}\right)^2\right] \quad (2)$$

where:

t_c = likely predicted comfort temperature (°C)
t_{out} = monthly mean outdoor temperature (°C)

ASHRAE [11] suggests that the acceptable mean monthly outdoor temperature should be between 10°C and 33.5°C for the effectiveness of this approach. The adaptive approach would be implemented in the remaining part of the project.

Chapter 3. Methodology

The first step in our methodology was to generate a load curve for the building for the whole year. To achieve this goal, the energy balance for the building was done to see the temperature variation of the building without using HVAC, and the heating or cooling load that would be required at any instant. The calculations were done for an average day of a month for the whole year i.e. a total of 12 days. The main terms considered for energy balance are conduction, convection, radiation, and internal heat generation.

3.1 Dimensions of the Building

For performing the energy balance, especially for the terms like conduction and radiation heat transfer, we need the correct dimensions and orientation of the building. The dimensions were taken online from google maps through the "Measure distance" option. The other details were taken from the drawings given by termofluids. The model of the building was made in Creo Software [20] to get the areas directly.

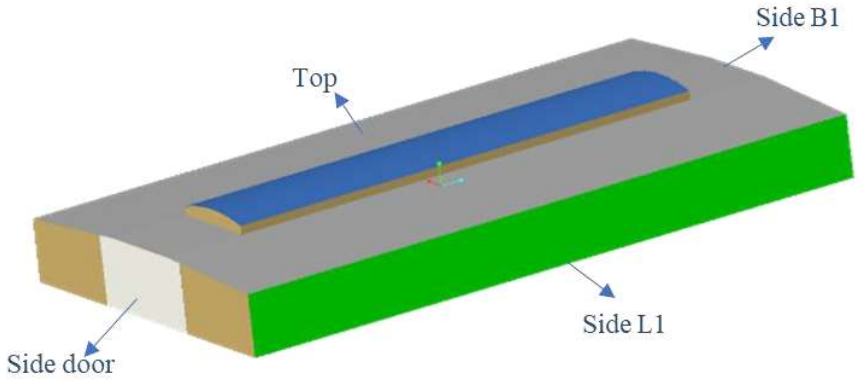

Figure 4 Dimensions of the building

Table 1 Areas of different Sides

Building Areas (m^2)	
L1	129
L2	129
Top	1092.55
B1_Nodoor	53.6
B2_Nodoor	53.6
Side door	29.6

3.2 Collection of Data

The very first step is to know the availability of solar radiation in the area. The office building for which we are designing the plant is located in the Terrassa region of Barcelona, Spain. The coordinates of the location are 41˚ 33' 49" and 2˚ 1' 24".

Figure 5 Satellite Image of the Office Building [21]

For this coordinate, the average daily Solar Irradiation and Ambient temperature data for an average day of each month of the year was gathered from the Online tool by European Commission called Photovoltaic Geographical Information System (PVGIS). The global solar irradiation for a plane surface is shown in Figure 6. This online tool made it easy because all we need is to put the slope and azimuth of the surface and we get the irradiance over that surface. The solar irradiance for all the four walls and the top surface were thus achieved.

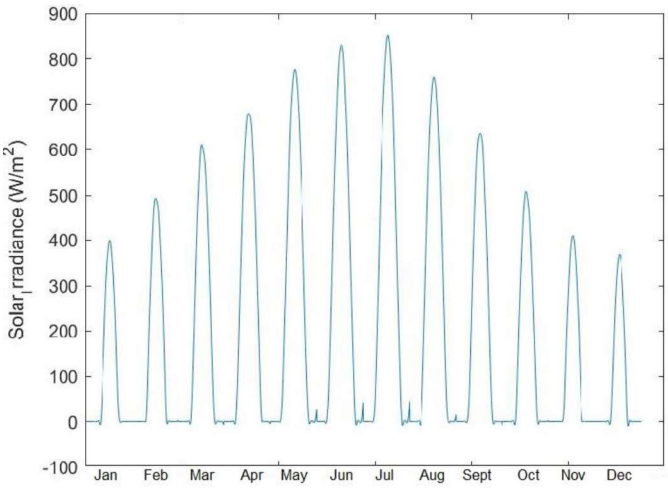

Figure 6 Solar Irradiance for average day of each month of the Selected Location

Similarly, the ambient temperature was also achieved as shown in Figure 7, from this online tool (PVGIS). This will be used in the calculation of conduction heat transfer. Since conduction heat transfer coefficient is dependent on the temperature difference.

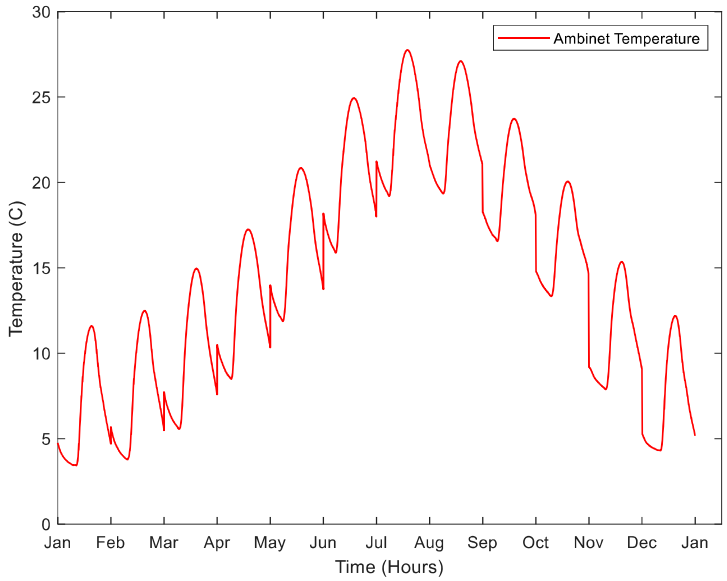

Figure 7 Ambient temperature profile of an average day of each month

3.3 Conduction and convection heat transfer

The computation of conduction and convection heat transfer was done together. For this, the UA value of each wall/surface was calculated. Then all were added together to be used in Equation 2 i.e. Newton's law of cooling

$$Q_C = (T_{ext} - T_{int}) \sum_i U_i A_i \tag{3}$$

Where T_{ext} is the ambient temperature (value got from PVGIS) and T_{int} is the room temperature, A_i is the surface area of each wall and $U_i = \frac{1}{R_{Total,i}}$. The calculation of the value of $R_{Total,i}$ for side L1(façade wall) is shown here for a sample.

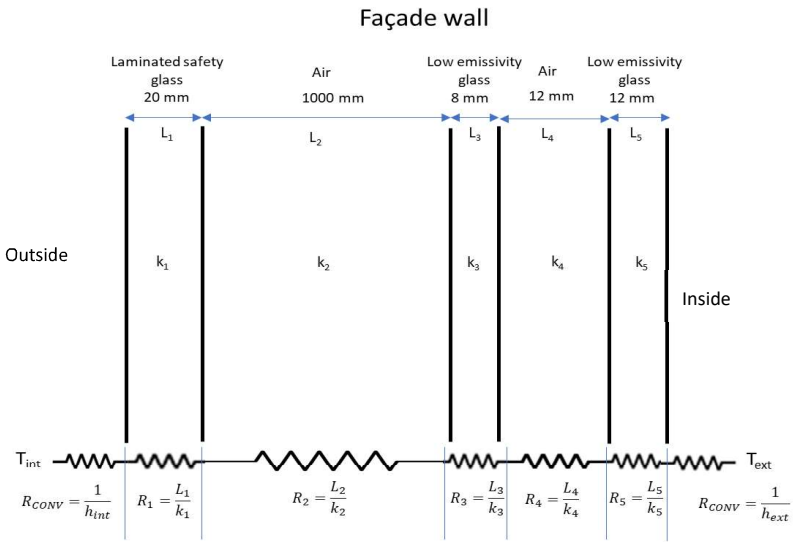

Figure 8 Resistances of facade wall (L1)

3.3.1 Calculation of resistance for wall

The façade wall has different layers of different materials. On the outside, it is air and a series of different glass layers with air trapped in between to provide better insulation. To calculate the total resistance, the conductivity and thickness of each layer of material were quantified. For the trapped air heat transfer coefficient was used for the given thickness. Thus the overall resistance was calculated by using equation 4.

$$R_{Total,i} = \frac{1}{h_{ext}} + \frac{1}{R_{1,i}} + \frac{1}{R_{2,i}} + \frac{1}{R_{3,i}} \dots \frac{1}{h_{int}} \quad (4)$$

3.4 Ventilation and infiltration heat transfer

No matter how much the building is sealed, there will still be some infiltration of air. The building has ventilated facades along its two sides. As a result, there will be replacement of air inside the building with fresh air from outside.

Heat transfer through ventilation was considered using the energy balance.

$$Q_V = C_p \rho V n (T_{ext} - T_{int}) \quad (5)$$

Where, C_p is the specific heat capacity of air, ρ is the density of air, V is the volume of the building which was computed using the Creo model and found to be 3828.93 m^3. The air change rate n, for office buildings, is taken as 0.5 per hour [22].

3.5 Radiative heat transfer

The amount of radiative heat transfer on the building is dependent on the amount of solar irradiation illuminating each surface throughout the day, the optical characteristics of the materials which made the surface, and the shading effect produced by the facades of nearby buildings. The following equation can be used to calculate the heat transfer rate.

$$Q_R = f_{sh} A_{sun} G_{sun} \quad (6)$$

Where, f_{sh} is the shading factor due to surrounding trees and buildings, as this building is located on the top floor, so the shading factor value was taken as 1. G_{sun} is the total solar irradiance (diffused + direct) illuminating each surface of the building depending on the azimuth and slope of the surface and time of the day (got from PVGIS) [23]. A_{sun} is the effective collecting surface whose value varies depending on the type of surface i.e. opaque or glazed.

3.5.1 Opaque surface

For opaque surfaces, A_{sun} is calculated by the equation 7 as:

$$\boldsymbol{A_{sun} = \frac{\alpha U A}{h_o}} \quad (7)$$

Where UA is the thermal transmittance calculated before while calculating the conduction term, α is the absorptance of the external surface. Where h_o is the outside thermal resistance.

3.5.2 Glazed surface

For glazed surfaces, A_{sun} is calculated by the equation 8 as:

$$\boldsymbol{A_{sun} = \tau A_{glazed}(1 - f_f)} \quad (8)$$

Where τ is the transmittance of the surface, A_{glazed} is the surface area of the glazed surface, f_f is the shading factor due to the green façade.

3.6 Internal heat generation

Internal heat generation (Q_g) in the building was also considered as this had a significant impact on the internal temperature of the room. The sources of heat generation considered were people and computers. The heat produced by lightning was neglected as very efficient lights are used in the building. As this was an office building, therefore 32 people were considered to be present in the building during office hours (8:00-18:00 hrs) and a desktop computer for each person was considered.

$$Q_g = N_{people} \times H_{person} + N_{appliance} \times H_{appliance} \quad (9)$$

Where, N_{people} and $N_{appliance}$ are the number of people and number of computers in the building and H_{person} and $H_{appliance}$ are the heats generated by each respectively.

Table 2 Heat sources of the building

Source	Generated Heat (Watts)
People	140 [24]
Desktop computer	70 [24]

3.7 Energy balance

A global energy balance was applied to the building, to compute the inside room temperature in the following way:

$$\rho C_P V \frac{\partial T}{\partial t} = Q_C + Q_V + Q_R + Q_g \quad (10)$$

The governing equation thus formed was then discretized by employing the Forward Euler Explicit method to obtain the room temperature throughout the day and the following discretized equation was obtained:

$$C \frac{T^{n+1} - T^n}{\Delta t} = (T_{ext}(t) - {T_{int}}^n) \sum_i U_i A_i + C_p \rho V n (T_{ext}(t) - {T_{int}}^n) + f_{sh} A_{sun} G_{sun}(t) + Q_g$$

Or

$$T^{n+1} = T^n + \frac{\Delta t}{C}\left((T_{ext}(t) - {T_{int}}^n) \sum_i U_i A_i + C_p \rho V n (T_{ext}(t) - {T_{int}}^n) + f_{sh} A_{sun} G_{sun}(t) + Q_g \right) \quad (11)$$

The term C in this equation takes into account the thermal inertia of the system which is dependent on the volume of the system, density, and specific heat capacity of the air inside.

$$C = \rho C_P V \quad (12)$$

Thus we can get the value of room temperature at the next time step if we know at the previous timestep. This equation was implemented in MATLAB to produce temperature variation of the building without HVAC as shown in Figure 9.The values for $G_{sun}(t)$ and $T_{ext}(t)$ were generated from the PVGIS website [23] and a considerably small timestep (Δt) of 1 second was taken in order to avoid convergence problems.

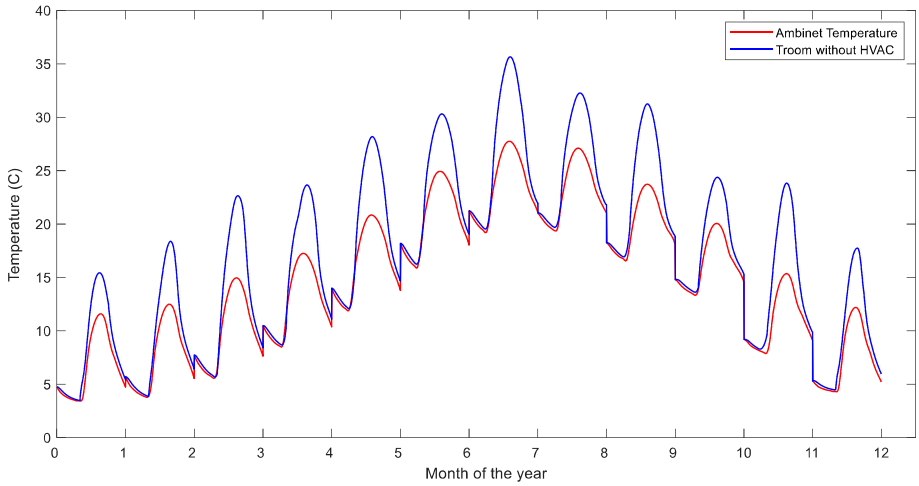

Figure 9 Room temperature without HVAC

3.8 Load Requirements

The next step was to get the HAVC load curve. The term 'HVAC' was added to equation 13 to model the heating or cooling supplied by the heat pump. The term will try to bring the temperature of the room to the thermal comfort required.

$$T^{n+1} = T^{n} + \frac{\Delta t}{C}\left((T_{ext}(t) - {T_{int}}^{n}) \sum_{i} U_i A_i + C_p \rho V n (T_{ext}(t) - {T_{int}}^{n}) + f_{sh} A_{sun} G_{sun}(t) + Q_g \pm HVAC \right) \quad (13)$$

3.8.1 Control System

The value of HVAC needs to be controlled because at different times different values of heating or cooling will be needed. A proportional control strategy was implemented for this system. This controller checks the temperature and the required comfort temperature at a given time step. The difference is then multiplied with a factor 'K' and then added to the previous HVAC load as shown in equation 14. The resulting values of HVAC load were then multiplied with a safety factor of 1.1 to be on the safe side.

$$HVAC(i+1) = HVAC(i) + K\left(T_{comf} - T_i\right) \quad (14)$$

Where T_{comf} is the comfort temperature that is calculated from the ambient temperature shown in equation 1.

After implementation in MATLAB, the final curves of temperatures and HVAC load are shown in Figure 10 and Figure 11 respectively. It should be noted that if the load curve is negative, it means cooling is required and vice version.

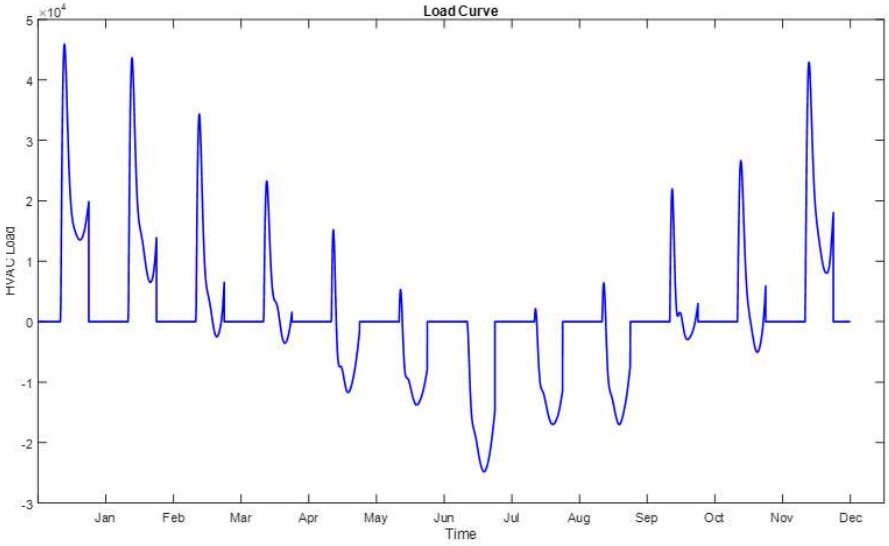

Figure 10 HVAC load Curve

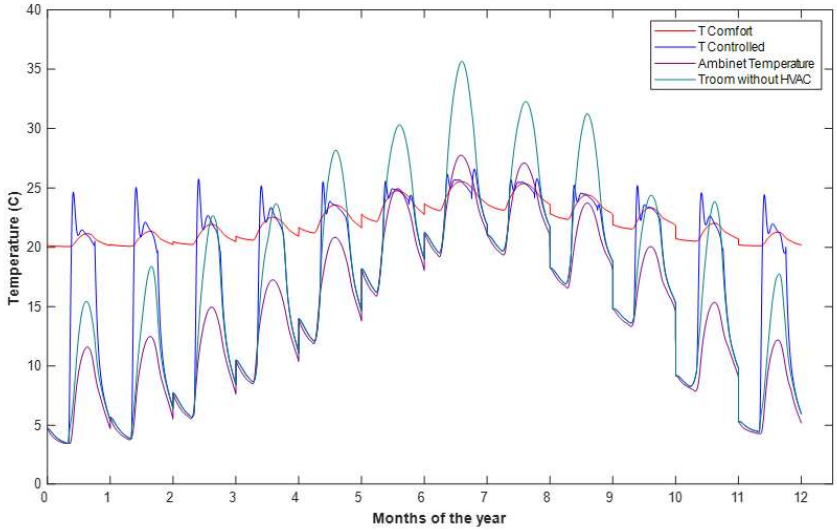

Figure 11 Effect of HVAC on the temperature

Chapter 4. Sizing and selection of the energy production plants

A solar-powered HVAC system aims to utilize the solar energy incident on a building for useful space-conditioning for the occupants. The solar-powered HVAC systems analyzed consist of two different types of layouts. The first one involves PV panels and a heat pump which is labeled as System A, and the second one involves solar collectors and an absorption chiller which is labeled as System B.

4.1 PV panel-based energy production plant (System A)

In a Photovoltaic (PV) panel-based energy production plant, solar energy from the sun will be converted into electrical energy which will then be used to power a heat pump to produce necessary heating or cooling for the building as required. As solar energy is intermittent, therefore a storage system is required to make up for times of less to no sunlight and therefore a battery storage system is also required. The configuration of system A has been shown in Figure 12.

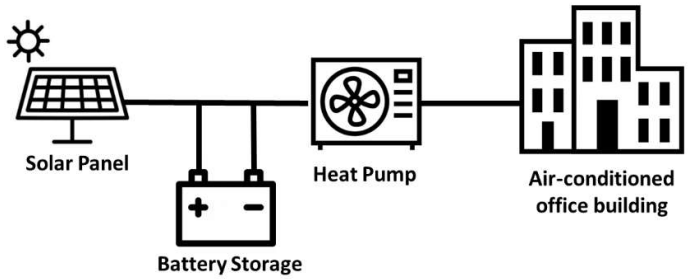

Figure 12 PV panel and heat pump-based energy production plant

4.2 Specifications of the components

For the design of the complete system, the properties of each component were specified based on their availability in the market.

The solar panels selected were monocrystalline since monocrystalline panels are more efficient as compared to polycrystalline panels [25]. The cost of the solar panel is decreasing with time. The price of a PV panel is 0.4 Euro/W. The major cost of the solar panel is their installation and relevant components needed like inverter, frames, and cables. This additional cost is estimated to be 0.5 Euro/W [26]. This makes the cost of a solar panel to be 0.9 Euro/W.

For the storage, the Lithium-Ion battery system was selected because of its wide availability in the market, high charge density, and lower self-discharge rate. The price of lithium-ion batteries nowadays is 332 Euro/kWh. [27]

For converting the electrical energy into heating or cooling, an air-to-air heat pump (ATAHP) was selected because air distribution with an air-to-air heat pump is more in line with the requirements of thermal comfort as compared to air-to-water heat pumps. [28] ATAHP can also be reversed to be used for providing cooling during the summer months. The heat pump chosen has a COP of 4.0 for heating and an EER of 3.3 for cooling.

4.3 Solar collector-based energy production plant (System B)

In solar thermal installations with large capacity, both solar cooling and solar heating are provided synergistically yielding a complete annual utilization. During the cold season, solar heat serves as space heating to maintain a comfortable temperature within the office space. During the warm season, solar heat is converted into cooling by utilizing absorption cooling devices to avoid overheating inside the office building.

The following figure shows the layout of the system B

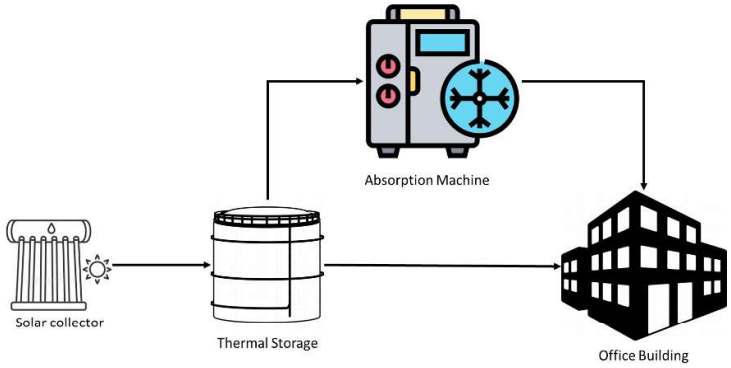

Figure 13 Solar collector and absorption chiller-based energy production plant

4.4 Specifications of the components

The selection of the thermal collector was based on the required inlet temperature of the absorption chiller. To select the type of collector to be used, the cost and performance of flat plate and evacuated tube collectors were compared. It was observed that though evacuated tube collectors are generally more efficient, they are mostly preferred in colder climates, and also are more expensive. Therefore, double-glazed flat plate collectors were decided to be used as the system would be used in a hot climatic region and they are also less expensive in contrast to the evacuated tube when considering the €/kWh. Their operating temperatures are in the range of 80 – 120°C. [29] For this, the solar collector chosen was Vitosol 200-FM manufactured by Viessmann. The cost of each panel is €701.40 and the aperture surface area for this panel is 2.33 m^2. [30]

For storage of the heat energy from the collectors, a thermal storage tank was introduced. During winter, the hot fluid from the tank would be channeled directly to a radiator in the building to provide heating. On the other hand, during summer, the building would be cooled by using an absorption chiller. For our system, Thermal Storage was considered that uses water as the fluid, and the cost of storage is €479.22/m^3 of storage volume.

Absorption chillers can be classified as single-effects, double-effects, and triple-effects. This means the number of times that heat is recycled in the chiller to produce cooling. These classifications are based on the operating temperatures and the nominal cooling capacity that would be used. The absorption chiller selected was the single-effect type as this was desirable considering the low-level operation temperature which could be achieved with the selected solar collector as compared to the other ones.

Table 3 Technical comparison for absorption chiller [29]

	Single-effect	Double-effect	Triple-effect
Heat source temperature	80 °C – 100 °C	180 °C	210 °C – 240 °C
Efficiency	0.7 – 0.8	1.4	1.8
Nominal cooling capacity (kW)	~5 – 10,000	~20 – 10,000	~350 – 10,000

For this system, a Li-Br-based Absorption Chiller was chosen, for which the COP is around 0.7. [31] The price of the chiller was €1320/kWh. [32]

4.5 Optimization

For comparing both systems, the production plants had to be sized. The sizing of the systems was done by implementing a Genetic Algorithm to optimize the number of PV panels and batteries in case of system A and the number of solar thermal collectors and capacity of the thermal storage tank in case of system B. A MATLAB code was formulated to apply the genetic algorithm for optimization purposes. The temperature profile, solar irradiance, and load profile (previously generated) were taken as input data. Component specifications were also taken as input data from commercially available component datasheets.

4.5.1 Optimization algorithm of PV Plant (System A)

The components of the system (PV panels, converters, and battery) were first modeled. PV panel production capacity was calculated using the following equation

$$P_{PV} = N_{PV}.\eta_{PV}.\frac{P_{PV}(STC) * G(SR)}{G(STC)}.\left(1 - CT.(T_{PV} - T_{STC})\right) \quad (15)$$

Where, N_{PV} is the number of the PV panels, η_{PV} is the electrical efficiency of PV panel, $P_{PV}(STC)$ is the power of the one PV panel under standard temperature conditions, $G(SR)$ is the Solar radiation in an incident on each wall of the building, $G(STC)$ is solar radiation under standard temperature conditions, CT is the temperature coefficient for calculating the effect of the difference between the temperature of the location and standard temperature conditions, T_{PV} is the temperature at the location of the building, $T_{STC} = 25°C$ are the standard temperature conditions (STC).

The converters were only modeled by using their respective efficiencies i.e., DC-DC converter efficiency $\eta_{DC/DC}$, DC-AC converter efficiency $\eta_{AC/DC}$.

The battery storage system was modeled by its state of charge (SOC) using the following equation:

$$SOC(t + \Delta t) = SOC(t) - \eta_{bat}.\left(\frac{P_{bat}}{N_{cell} \times C_{cell}}\right).\Delta t \quad (16)$$

Where, SOC is the state of charge of the battery, η_{bat} is the efficiency of the battery, P_{bat} is the power of the battery (charging and discharging), N_{cell} is the number of battery cells and C_{cell} is the capacity of each cell.

- A control strategy was then applied to decide the amount of power that went to the battery and to supply the load. The constraints applied to the control system were as follows:
- The state of the charge of the battery should always be between the defined minimum and maximum states of charge.

- There should be zero unsupplied loads to make sure there is no blackout at any time

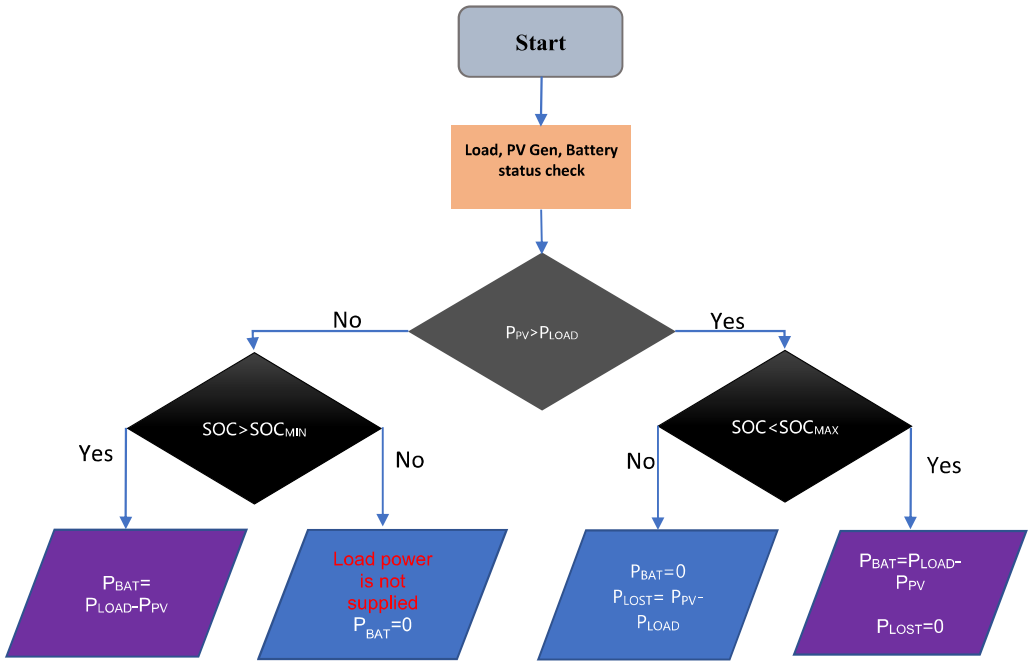

Figure 14 Control strategy applied on PV plant

The final step was to write the objective function. The objective function is the function that has to be minimized. In our case, the cost of the components involved in the system was minimized. The objective function used is given below:

$$Cost = N_{PV}.Cost_{PV} + N_{bat}.Cost_{bat} \quad (17)$$

The cost of the whole system was calculated by multiplying the cost of a single battery and PV panel by the number of batteries and PV panels used respectively. The genetic algorithm decided what were the best values for variables such as the number of PV panels, the number of the battery cells, and the initial value of SOC of the battery to minimize the cost of the system.

4.5.2 Optimization algorithm of the solar collector plant (System B)

Like the PV plant, the solar collector plant was optimized for its sizing. To model the plant, the efficiency of the collectors was obtained from the manufacturer's catalog (Viessmann), and the thermal power gain, P_{SC} was obtained using the relation:

$$P_{SC} = N_{sc}.\eta.A.I \quad (18)$$

where N_{SC} is the number of solar collectors, η is the collector efficiency, A is the surface area of the collector, and I is the direct solar irradiation.

To design the thermal tank, a control strategy of the temperature was set to enable the adequate temperature needed for the absorption chiller (70-80 °C) to be maintained. To determine the energy that would be required from the tank for heating or cooling, the following was used:

$$COP = \frac{|Q|}{W} \quad (19)$$

where COP is the coefficient of performance of the absorption chiller or radiator, Q is the heating or cooling required and W is the input energy from the thermal storage tank/solar collector.

The objective function was to minimize the cost of the components that were used, and the function is given as:

$$Cost = N_{SC}.C_{SC} + V_{ST}.C_{ST} \quad (20)$$

Where N_{SC} is the number of the solar collectors, C_{SC} is the unit price of the flat plate collector, V_{ST} is the volume of the storage tank and C_{ST} is the unit cost of the storage tank.

The following constraints are provided to the optimization algorithm

$$4 < N_{SC} < 500$$

$$1m^3 < V_{ST} < 10m^3$$

$$70°C < T_{tank} < 80\,°C$$

The temperature change inside the tank is given by the following equation

$$T(k+1) = T(k) + \frac{\eta_{tank}.P_{tank}(k).deltaT}{Volume.Cp.density} \quad (21)$$

&

$$Ptank(k) = \eta_{sc_{tank}}.\left(P_{sc(k)} - P_{load(k)}\right) \quad (22)$$

Where η_{tank} is the efficiency of the tank and $\eta_{sc_{tank}}$ is the efficiency of the heat transfer from the solar collector to the tank.

In the end, the required number of collectors, volume of the tank, and initial temperature were obtained. The following flowchart shows the strategy used for the optimization of the solar collector plant.

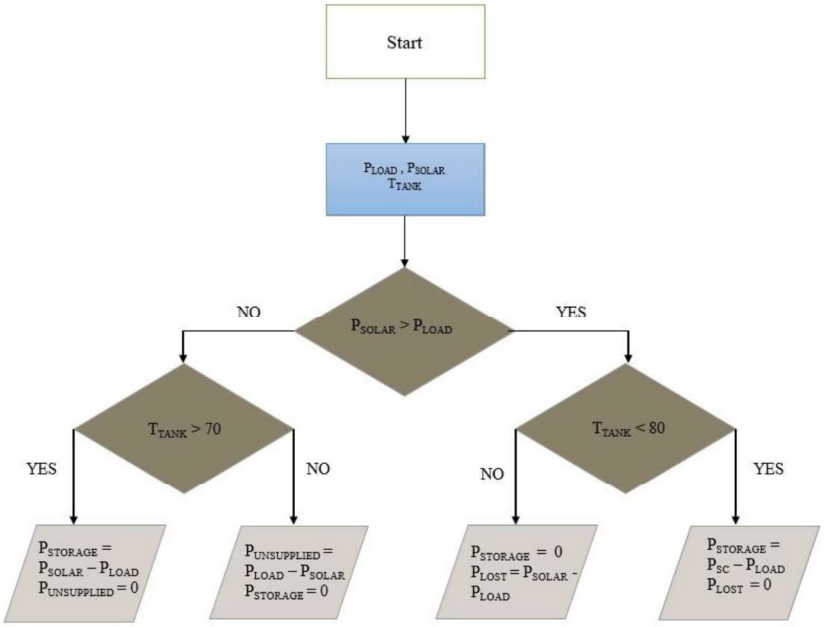

Figure 15 Control strategy applied on solar thermal plant

4.6 Optimization Results

The optimization algorithm precisely computes the system requirements. Application of genetic algorithm provided the sizes of each energy production plant indicating the optimal number of PV panels/solar collectors and batteries/thermal storage required to meet the load demand at all times along with their cost. The algorithm does not only consider the load requirements rather it takes into account the cost factor too.

Optimization was performed for an average day of each month over the whole year. The following table shows the optimization results of both plants

Table 4 Optimization results

	Quantity	Cost (€)
PV Panels	46	16,974.00
Batteries	25	45,800.00
Heat Pump	1	28,715.00
System A Total Cost (€)	**91,489.00**	
Solar Collectors	73	51,202.20
Thermal Storage (m^3)	10	4,792.20
Absorption Chiller	1	66,000.00
System B Total Cost (€)	**121,994.40**	

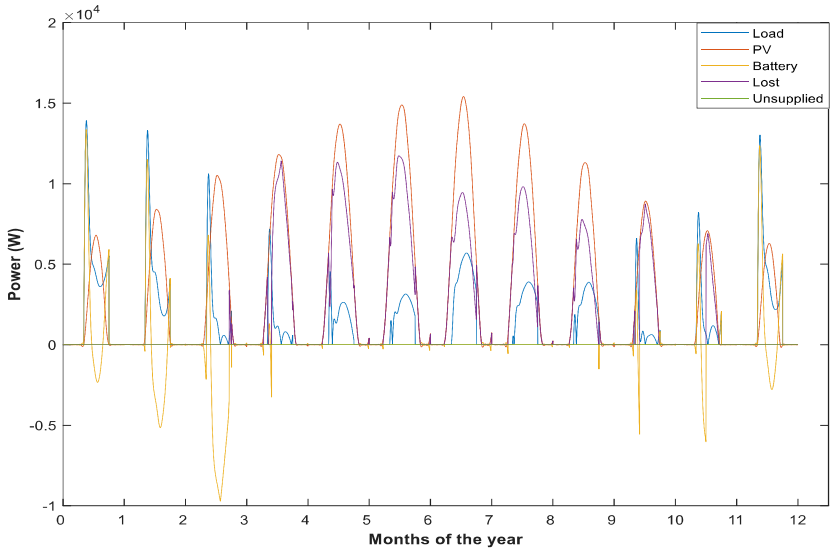

Figure 16 Optimization of system A with batteries

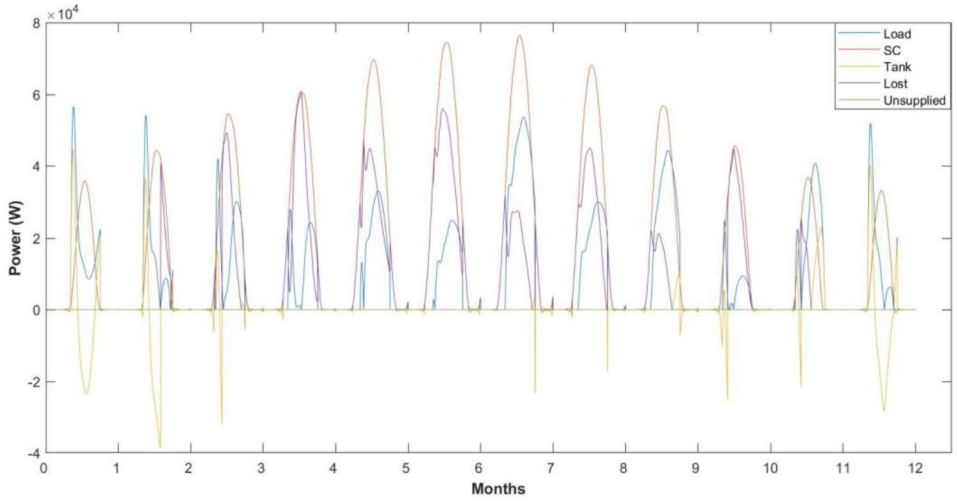

Figure 17 Optimization of system B with Thermal Storage

Comparison of system A and system B

A comparison of both energy production plants was then carried out based on the levelized cost of energy, system efficiency, life span, and their environmental impacts.

4.6.1 Levelized energy cost

One of the major parameters while comparing energy production plants is the cost of a unit of energy. So a levelized energy cost comparison was made incorporating capital investment, operational cost, and considering the life span of each plant.

4.6.1.1 Methodology of LCOE, LCOC & LCOH Calculation

First, the total amount of energy this plant will consume for the given system is calculated by using the data of the load profile. It was assumed that the temperature profile of each year will remain the same. The total energy consumed with degradation of 0.25% was calculated.

Next, the total cost of the energy production plant using PV was calculated for 25 years [33]. The cost of the different components used has already been mentioned in 4.2. Using those costs the computation of the total capital cost was done as stated below.

$$Total\ life\ cost\ =\ Capital\ Cost\ +\ Operational\ Cost \tag{23}$$

Whereas for system A,

$$Capital\ Cost = Cost\ of\ (PV + Batteries + Installation) \tag{24}$$

And for system B,

$$Capital\ Cost = Cost\ of\ (Solar\ Collectors + Thermal\ storage\ tank\ +\ Installation) \tag{25}$$

The levelized cost of energy was then calculated by the formula

$$LCOE = \frac{Total\ Life\ cost}{Total\ Energy\ Consumption} \tag{26}$$

The problem with LCOE is that for system A, it is the cost per unit of electricity while for system B, it is the cost per unit of heating. So this number was converted to levelized cost of cooling (LCOC) and levelized cost of Heating (LCOH) by multiplying it by a factor of f.

$$LCOC, LCOH = f \times LCOE \quad (27)$$

Where f is a factor that takes into account all the losses or COP from source till the building. The value of f is different for LCOC and LCOC. Thus to make a fair comparison between the two plants, the cost per kW of cooling and heating produced from both plants was calculated.

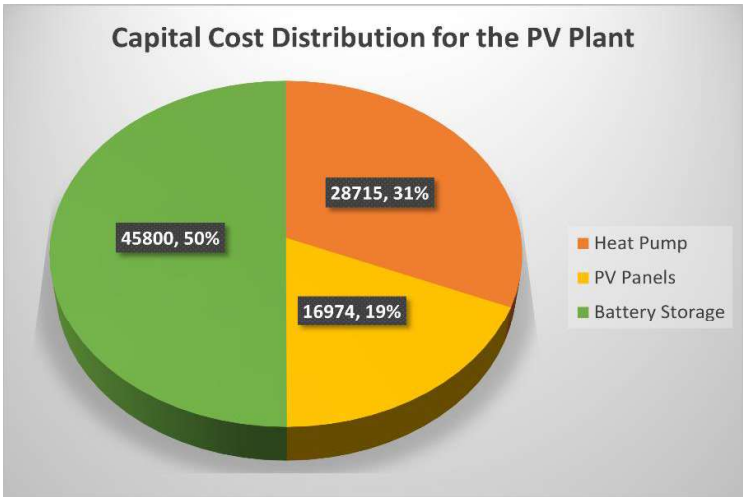

Figure 18 Share of each factor in System A total cost

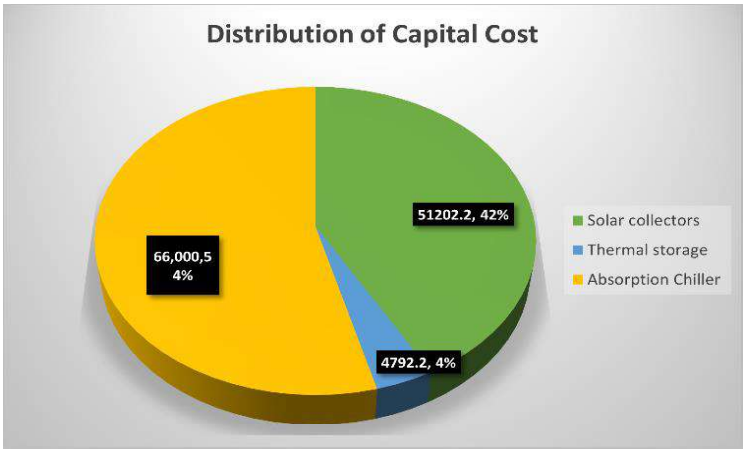

Figure 19 Share of each factor in System B cost

Table 5 Costs associated with both plants

Production Plant	Capital Cost	Operating Cost	Life Span	LCOE	LCOC	LCOH
	(€)	(€/year)	(Years)	(€/kWh)	(€/kWh)	(€/kWh)
System A	91,489.00	822.22	25	0.16*	0.06	0.05
System B	121,994.40	279.97	25	0.04**	0.1	0.06

Where * represents Electrical energy and ** represents thermal energy

4.6.1.2 Capacity Utilization Factor

The CUF of both systems was then calculated to gauge the performance of the systems

$$CUF = \frac{E_{plant}}{C_{peak} \times hours \times days} \tag{28}$$

Where E_{plant} is the actual energy output of the plant per year (kWh/year) and C_{peak} is the peak capacity of the plant (kW).

Table 6 CUF of each system

Energy Production Plant	Capacity Utilization Factor (%)
System A	17.5
System B	18.8

4.6.2 Break-even point/payback time

As per the stats available on the websites of the PV manufacturing companies, the average life span of the PV system range from 25-35 years [33]. The PV panels used are of the SUNPOWER COMPANY and it guarantees 25 years of life span for the respective PV setup. So here we assume that the life span of our system is 25 years and based on that we proceed with the calculations of LCOE, Capacity Utilization, and break-even point. The life span of solar collectors is also around 25 years. [34]

The break-even analysis has been done considering the degradation factor of 0.25% per year as stated by the manufacturing company. The graphical analysis has been shown below, the PV plant pays back its cost in roughly 16 years, whereas the solar collector plant takes 17 years.

The cost of electricity used for break-even analysis is 0.24 euro/kWh which is the cost of electricity in Barcelona Spain and the cost of thermal heating was 0.061 euro/kWh [35].

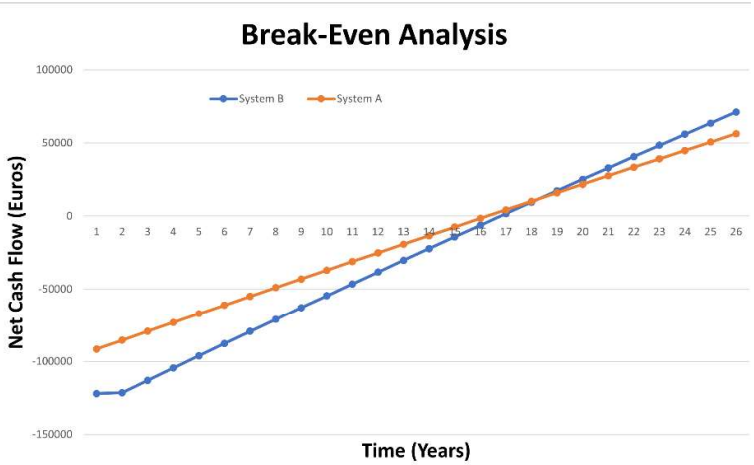

Figure 20 Break-Even analysis of both the plants

4.6.3 Carbon Savings

To assess the environmental impacts of both plants, their life cycle assessment studies were considered. Since both systems use solar energy, there are no direct emissions obtained from the generation of electricity and thermal energy of the plants during their operation. To quantify the effect of CO_2 emissions concerning the plants, we considered the amount of CO_2 that would be saved by the usage of either of the plants. In Spain, for electricity and heat generation from the grid, 198 gCO_{2eq}/kWh is generated [36]. The total electrical energy produced per year in the plant is 28,910 kWh and with this, an emission saving of 5.72 tonne of CO_2 per year would be achieved. Over the entire lifespan of the plant (25 years), an emission saving of 143 tonnes of CO_2 would be accomplished.

Chapter 5. Conclusion

One of the main criteria for designing a green building is the use of clean energy, and for the HVAC system of the office building in question, solar energy is to be used. In this study, a genetic algorithm was used to generate and compare the costs between two different solar-based energy production plants. One of the plants relies on PV panels and Lithium-ion batteries for producing and storing electrical energy and generates heating and cooling using a heat pump. The other plant relies on solar collectors and thermal energy storage for producing and storing thermal energy and generates heating directly from the thermal storage tank and cooling using an absorption chiller.

An analysis of different economic and environmental criteria included the capital investment, levelized cost of cooling, and break-even point. It was observed that for the PV system, most of the investment costs (about 50%) would be spent on the batteries, whereas for the solar collector system about 54% of the investment costs would be spent on the Absorption Chiller. Furthermore, the capital cost and the break-even period for system A proved to be better than that of system B which were approximately 16 years and 17 years respectively.

With the comparisons based on the aforementioned criteria, the PV-based plant (System A) was selected as a better choice having an LCOE of 0.16 €/kWh for a 25 years lifetime.

Considering the selection of a system for the heating and cooling of the building, the next phase of the project would entail a detailed analysis of each of the required components in a 0D/1D dynamic approach using the OpenModelica platform.

Chapter 6. Bibliography

[1] "The Future of Cooling – Analysis, IEA," [Online]. Available: https://www.iea.org/reports/the-future-of-cooling. [Accessed 15 May 2022].

[2] "What is green building?," World Green Building Council, [Online]. Available: https://www.worldgbc.org/what-green-building. [Accessed 15 May 15 2022].

[3] J. Khan, "Evolution to Emergence of Green Buildings: A Review," *Administrative Sciences,* vol. 9, no. 1, p. 6, Jan. 2019, doi: 10.3390/admsci9010006.

[4] A. Chel and G. Kaushik, "Renewable energy technologies for sustainable development of energy efficient building," *Alexandria Engineering Journal,* vol. 57, no. 2, p. 655–669, Jun. 2018, doi: 10.1016/j.aej.2017.02.027..

[5] A. Aksamija, "Regenerative Design of Existing Buildings for Net-Zero Energy Use," *Procedia Engineering,* vol. 118, p. 72–80, 2015, doi: 10.1016/j.proeng.2015.08.405.

[6] X. Cao, X. Dai and J. Liu, "Building energy-consumption status worldwide and the state-of-the-art technologies for zero-energy buildings during the past decade," *Energy and Buildings,* vol. 128, p. 198–213, Sep. 2016, doi: 10.1016/j.enbuild.2016.06.089.

[7] M. Borrallo-Jiménez, M. LopezDeAsiain and P. M. Esqui, "Comparative study between the Passive House Standard in warm climates and Nearly Zero Energy Buildings under Spanish Technical Building Code in a dwelling design in Seville, Spain," *Energy and Buildings,* vol. 254, p. 111570, Jan. 2022, doi: 10.1016/j.enbuild.2021.111570.

[8] M. A. Kamal, "An Overview of Passive Cooling Techniques in Buildings: Design Concepts and Architectural Interventions," *Civil Engineering,* vol. 55, no. 1, p. 15, 2012.

[9] L. e. a. Belussi, "A review of performance of zero energy buildings and energy efficiency solutions," *Journal of Building Engineering,* vol. 25, p. 100772, Sep. 2019, doi: 10.1016/j.jobe.2019.100772.

[10] L. F. Cabeza, D. Urge-Vorsatz, M. A. McNeil, C. Barreneche and S. Serrano, "Investigating greenhouse challenge from growing trends of electricity consumption through home appliances in buildings," *Renewable and Sustainable Energy Reviews,* vol. 36, p. 188–193, Aug. 2014, doi: 10.1016/j.rser.2014.04.053.

[11] "ANSI/ASHRAE Standard 55-2010," *Thermal Environmental Conditions for Human Occupancy,* p. 44, 2010.

[12] A. S. o. H. R. a. A.-C. E. I. (ASHRAE), "2021 ASHRAE Handbook - Fundamentals. 2021.".

[13] N. Djongyand, R. Tchinda and D. Njomo, "Thermal comfort: A review paper," *Renewable and Sustainable Energy Reviews,* vol. vol. 14, no. 9, p. 2626–2640, Dec. 2010 doi: 10.1016/j.rser.2010.07.040.

[14] D. Enescu, "A review of thermal comfort models and indicators for indoor environments," *Renewable and Sustainable Energy Reviews,* vol. vol. 79, p. 1353–1379, Nov 2017, doi: 10.1016/j.rser.2017.05.175.

[15] N. Ma, D. Aviv, H. Guo and W. W. Braham, "Measuring the right factors: A review of variables and models for thermal comfort and indoor air quality," *Renewable and Sustainable Energy Reviews,* vol. vol. 135, p. 110436, Jan. 2021, doi: 10.1016/j.rser.2020.110436.

[16] J. A. Orosa Jose, "A Review of General and Local Thermal Comfort Models for Controlling Indoor Ambiences," 2010. doi: 10.5772/9763.

[17] S. Guenther, "What Is PMV? What Is PPD? Basics of Thermal Comfort," SimScale, 3 September 2019. [Online]. Available: https://www.simscale.com/blog/2019/09/what-is-pmv-ppd/. [Accessed 18 June 2022].

[18] N. Ma, D. Aviv, H. Guo and W. W. Braham, "Measuring the right factors: A review of variables and models for thermal comfort and indoor air quality," *Renewable and Sustainable Energy Reviews,* vol. 135, p. 110436, Jan. 2021, doi: 10.1016/j.rser.2020.110436.

[19] M. Humphreys and J. F. Nicol, "Understanding the adaptive approach to thermal comfort," 1998.

[20] P. T. Corporation, *Creo 5.0 software,* Boston: PTC, 2018.

[21] *Google Earth Pro,* 2022.

[22] V. Giacomo, C. Peretti, S. Gracl and M. D. Carl, "Building leakage analysis and infiltration modelling for an italian multifamily building," *Journal of Building Performance Simulation,* vol. 6, no. 2, pp. 98-118, 2013.

[23] "PHOTOVOLTAIC GEOGRAPHICAL INFORMATION SYSTEM," Joint Research Center, [Online]. Available: https://re.jrc.ec.europa.eu/pvg_tools/en/. [Accessed 5 May 2022].

[24] Y. A. Çengel, Heat Transfer-A practical approach, McGraw-Hill, 2003.

[25] C. E. C. Nogueira, J. Bedin, R. K. Niedzialkoski, S. N. Melegari de Souza and J. C. Munhoz das Neves, "Performance of monocrystalline and polycrystalline solar panels in a water pumping system in Brazil," *Renewable and Sustainable Energy Reviews,* vol. 51, pp. 1610-1616, 2015.

[26] A. Aalik and A. Annuk, "An alternative approach to the feasibility of Photovoltaic Power Stations in light of falling PV Panel Prices," Paris, France, 2018.

[27] A. Mayyas, A. Chadly, S. Talib Amer and E. Azar, "Economics of the Li-ion batteries and reversible fuel cells as energy storage systems when coupled with dynamic electricity pricing schemes," *Energy,* vol. 239, 2022.

[28] B. Xiao, L. He, S. Zhang, T. Kong, B. Hu and R. Wang, "Comparison and analysis on air-to-air and air-to-water heat pump," *Renewable Energy,* vol. 146, pp. 1888-1896, 2019.

[29] A. Shirazi, R. A. Taylor, G. L. Morrison and S. D. White, "Solar-powered absorption chillers: A comprehensive and critical review," *Energy Conversion and Management,* vol. 171, p. 59–81, Sep. 2018, doi: 10.1016/j.enconman.2018.05.091.

[30] "Viessmann Vitosol 200-FM," Viessmann, [Online]. Available: https://www.viessmann.fr/fr/chauffage-maison-individuelle/solaire-thermique/capteur-plat/vitosol-200-fm.html. [Accessed 21 6 2022].

[31] J. Deng, R. Wang and G. Han, "A review of thermally activated cooling technologies for combined cooling,," *Progress in Energy and Combustion Science,* p. 198, 2011.

[32] "PURIX," Purix, [Online]. Available: https://www.purix.com/. [Accessed 14 4 2022].

[33] R. H. Wiser, M. Bolinger and J. Seel, "Benchmarking Utility-Scale PV Operational Expenses and Project Lifetimes: Results from a," Lawrence Berkeley National Laboratory, California, 2020.

[34] "Yougen UK," [Online]. Available: https://yougen.co.uk/2011/11/07/solar-thermal-a-guide-to-life-expectancy-and-maintenance/. [Accessed 19 6 2022].

[35] "Global Petrol Prices," -, - March 2022. [Online]. Available: https://www.globalpetrolprices.com/Spain/electricity_prices/#:~:text=Spain%2C%20September%202021%3A%20The%20price,of%20power%2C%20distribution%20and%20taxes.. [Accessed June 2022].

[36] "Spain 2021 Energy policy review, International Energy Agency".

[37] S. Solar Absorptances and Spectral Reflectances of 12 Metals for TemperatErnie W, W. Albert J, B. Robert L and J. John R, "Solar Absorptances and Spectral Reflectances of 12 Metals for Temperatures Ranging from 300 to 500K," NATIONAL AERONAUTICS AND SPACE ADMINISTRATION, Washington D.C., 1969.

Appendix A

Building Drawings, Dimensions, and Material Properties

Building Drawings

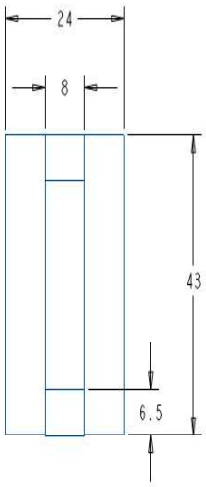

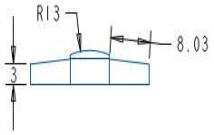

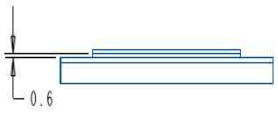

	Building				
Checked By		Drawing title	DRAWING	Scale	0.002
Drawn_by	Izaz Gul	Model name	PRT0001	Size	A3
Session:		Model type	PART	Units	m

For Thermal Resistance Calculations

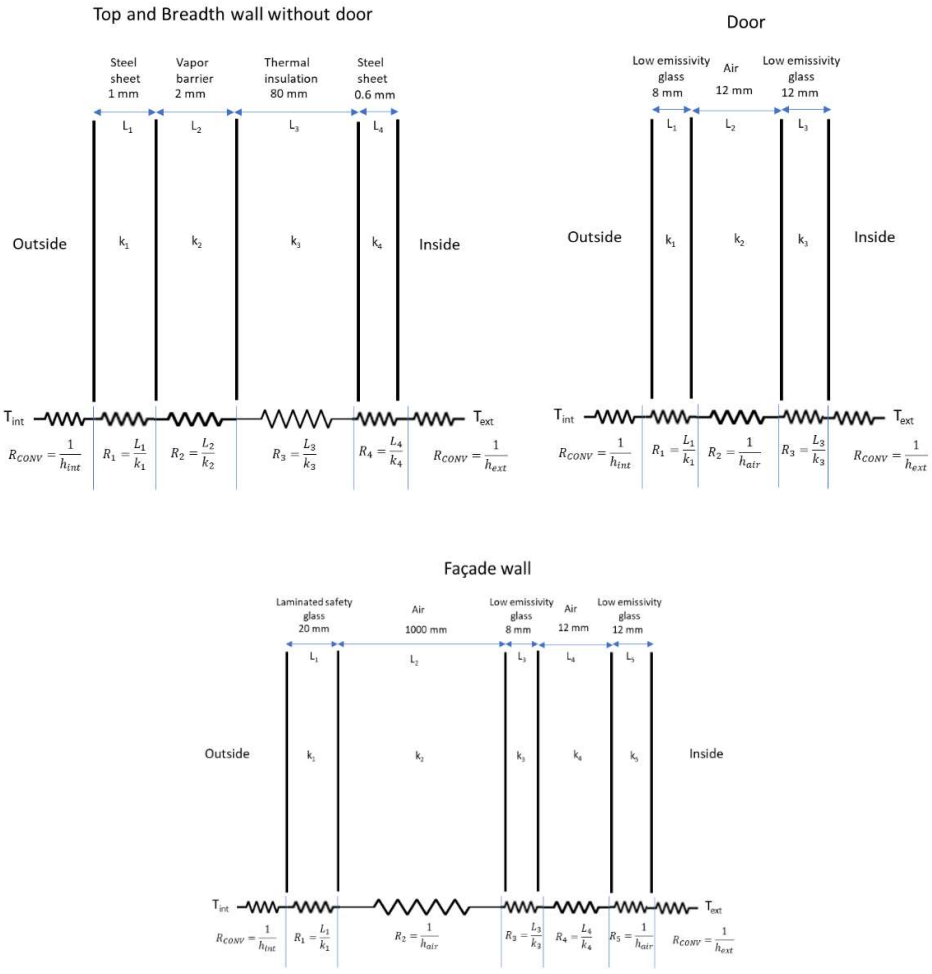

Building material properties

Material	Thermal Conductivity W/(m·K)
Steel sheet	45
Vapor barrier	0.4
Thermal insulation (rock wool)	0.044
Laminated safety glass	1
Low emissivity glass	1
Material	**Heat Transfer Coefficient**
Façade Air	6.25 [24]
Inside Air	8.29 [24]

Glazed surface properties

Material	Absorptance
Steel	0.354 [37]
Material	**Transmittance**
Low emissivity glass	0.35